Article

Study on Valve Strategy of Variable Cylinder Deactivation Based on Electromagnetic Intake Valve Train

Maoyang Hu, Siqin Chang *, Yaxuan Xu and Liang Liu

School of Mechanical Engineering, Nanjing University of Science and Technology, Nanjing 210094, China; humaoyang@126.com (M.H.); njustxyx@gmail.com (Y.X.); liuliang@njust.edu.cn (L.L.)

* Correspondence: changsq@mail.njust.edu.cn; Tel.: +86-025-84315451

check for updates

Abstract: The camless electromagnetic valve train (EMVT), as a fully flexible variable valve train, has enormous potential for improving engine performances. In this paper, a new valve strategy based on the electromagnetic intake valve train (EMIV) is proposed to achieve variable cylinder deactivation (VCD) on a four-cylinder gasoline engine. The 1D engine model was constructed in GT-Power according to test data. In order to analyze the VCD operation with the proposed valve strategy, the 1D model was validated using a 3D code. The effects of the proposed valve strategy were investigated from the perspective of energy loss of the transition period, the mass fraction of oxygen in the exhaust pipe, and the minimum in-cylinder pressure of the active cycle. On the premise of avoiding high exhaust oxygen and oil suction, the intake valve timing can be determined with the variation features of energy losses. It was found that at 1200 and 1600 rpm, fuel economy was improved by 12.5–16.6% and 9.7–14.6%, respectively, under VCD in conjunction with the early intake valve closing (EIVC) strategy when the brake mean effective pressure (BMEP) ranged from 0.3 MPa to 0.2 MPa.

Keywords: variable cylinder deactivation; EMVT; valve strategy; energy losses; fuel economy

1. Introduction

Since throttle can restrict the air from flowing into the cylinders, pumping mean effective pressure (PMEP) is high at part load conditions for throttled internal combustion engines. Cylinder deactivation (CDA) has been demonstrated to be a reliable technology for improving fuel economy in gasoline engines under low load conditions at low and middle speed. When some of the cylinders are deactivated, the remaining firing cylinders require more air and fuel to maintain the same BMEP level. Therefore, the throttle angle is increased and the pumping losses are reduced due to higher intake manifold pressure [1,2], and combustion is generally more complete with larger air-fuel charge motion. Moreover, when the intake and exhaust valves are deactivated, the deactivated cylinder acts as an air spring, repeatedly compressing and expanding the same air. The air spring losses are very low [2,3]; approximately 0.02 bar indicated mean effective pressure (IMEP).

Leone et al. found that CDA had the greatest potential to improve fuel economy for large engine sizes relative to vehicle weight, with fuel economy being improved by 6 to 11% for V8 and V10 engines [3]. The Active Fuel Management (AFM) system was included in the 3.9 L V6 engine and improved fuel consumption by 5.5–7.5% without compromising engine performance [4]. In recent years, with the restriction of environmental regulations and the wide application of small displacement turbocharged engines [5], more and more CDA technologies have been applied to small displacement engines [2,6]. Mohd Abas et al. [2] found that CDA improved fuel consumption by 6 to 25% for

a 1.6 L in-line 4-cylinder gasoline engine when cylinders 2 and 3 were shut. VW has introduced CDA technology on a 1.4 L 4-cylinder TSI engine by switching the cam lobes between normal profiles and zero lift when the CDA mode was implemented [7].

In addition to the fixed two CDA modes above, three fixed-mode CDA technologies also have been developed. HONDA developed the new Variable Cylinder Management (VCM) system on a 3.5 L V6 engine. The newly developed VCM system introduces a four-cylinder mode to the conventional three-cylinder and six-cylinder modes, and makes it possible to switch between the three modes to increase practical fuel economy [8]. Moreover, the three-mode (L4-L3-L2) CDA technology was also introduced in a 1.1 L in-line four-cylinder motor engine [9]. Yaojung Shiaoa et al. [10] studied the three-mode (L4-L3-L2) CDA technology on a 4-cylinder engine based on an unthrottled spark ignition (SI) engine with electromagnetic valve train, and found that the improvement in fuel consumption was about 7 to 21%. Compared with traditional fixed two-mode CDA technology, three-mode CDA can improve fuel economy further with the appropriate number of cylinders according to engine conditions.

In addition to CDA, EIVC and late intake valve closing (LIVC) are also effective methods to reduce PMEP [11–13]. By combining CDA with EIVC or LIVC, PMEP can be minimized further. Millo et al. [6] investigated the benefits of fixed two-mode (L4-L2) CDA on a four-cylinder unthrottled engine equipped with a MultiAir system. The authors developed an innovative CDA valve strategy that combines internal Exhaust Gas Recirculation (iEGR) with EIVC. The results demonstrated a 30% reduction in pumping losses, and an 8% improvement in fuel efficiency compared with the condition of only EIVC load control strategy. Jinxing Zhao et al. [5] proposed a novel CDA technology through double intake manifolds for four-cylinder SI engines. The results showed that after combining the CDA with LIVC, the pumping loss decreased by 58.9–65.6% and 24.5–35.3% at 2000 rpm and 4000 rpm, respectively.

In addition to the combination of fixed CDA technology with EIVC or LIVC, skip fire technology is also a more attractive CDA technology that can be classified into two categories: fixed skip fire (FSF), and dynamic skip fire (DSF). Yuanping Zhao et al. [14] designed 23 FSF modes with firing density varying from 22 to 100%. Levent Yüksek et al. [15] investigated a cycle-skipping strategy on a single-cylinder engine. The three modes include N, NS, and NSS (N represents non-skipping while S represents skip cycle). However, the skip cycle is achieved by simply interrupting fuel injection and ignition in the skipped cylinders without any other modification to the valve train. The fresh air is sucked into the skipped cylinder and then discharged into the exhaust pipe, leading to high exhaust oxygen and decreased efficiency of the three-way catalysts. DSF strategy has no fixed mode, and makes it possible to change the load rate and the firing density in proportion to the torque demand [1]. Moreover, the resonant frequency of the drivetrain can be avoided at all engine speeds through the implementation of different firing patterns at different engine speed ranges [16,17]. The commonness of FSF and DSF is that every cylinder would perform as a firing cycle and skip cycle when the engine operates in skip fire condition. The difference is that DSF adjusts the firing density to keep pace with the continuously varying input torque demand, so that the firing cylinders can work in the high efficiency area, and the heat and mechanical balance of all the cylinders are mostly consistent.

In this study, the investigation focuses on the realization of a VCD operation that allows the firing density of the cylinder to vary from 50 to 100% continuously. Firstly, a new valve strategy based on EMIV without any modification to the exhaust valve is proposed to realize the VCD operation. Then, a 1D prototype engine model is constructed and calibrated using experimental data in GT-Power. The simulation model for the VCD engine with a EIVC strategy based on EMIV is further developed. In order to accurately analyze the distribution of exhaust gas and air in the intake manifold, the 1D model of VCD based on EMIV is tuned using the simulation results of the 3D code. After that, the effects of the proposed valve strategy on the mass fraction of oxygen in the exhaust pipe, the energy losses, and the minimum in-cylinder pressure of inactive cycle are investigated based on the simulation models. On the premise of avoiding high exhaust oxygen and oil suction, finally the intake valve opening timing (IVO) and intake valve closing timing (IVC) are determined by the minimum energy

losses of the inactive cycle. Correspondingly, the fuel benefits achieved by VCD are also analyzed at low load operations.

2. Test of the EMVT and Valve Strategy

2.1. Test of the EMVT

The self-developed [18] EMVT is a highly flexible camless valve train system that offers flexible variable valve timing, valve duration, and valve lift, which provides a feasible approach to actualizing the CDA strategy. Through several updates, the EMVT has met the requirements of fast transition time, low impact velocity, and low power consumption. It has been proved that the EMVT has great potential for improving engine performance. At present, the EMVT has been installed on the intake side without any modifications to the exhaust valves. As shown in Figure 1, the test bench of the engine cylinder head with the EMIV has been completed.
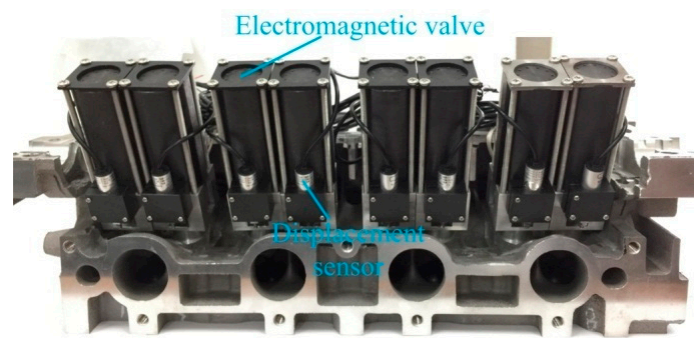

Figure 1. Test bench of engine cylinder head with EMVT.
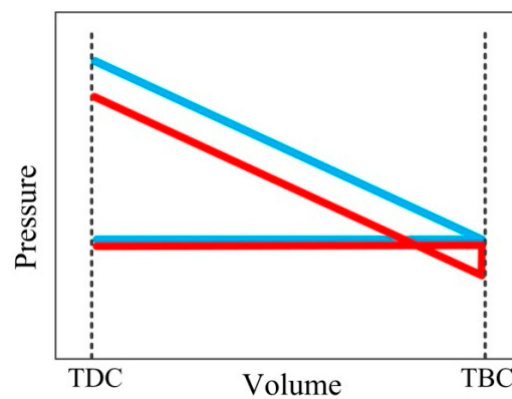
2.2. Valve Strategy

The charge trapped in the inactive cylinder of the CDA operation usually includes fresh air, low-pressure charge (deactivation of a cylinder after its exhaust event), and exhaust gas. Based on EMIV without any modification to the exhaust valves, three valve strategies based on fresh air trapping, low-pressure charge, and exhaust gas trapping are proposed. The schematic of the valve strategy for fresh air trapped during one active cycle and one inactive cycle is shown in Figure 2. The fresh air is first sucked into the inactive cylinder during the intake stroke of the inactive cycle. At the end of the inactive cycle, the exhaust valve event occurs normally, and thus the fresh air is released into the exhaust manifold. The schematic of the in-cylinder pressure during the inactive cycle is shown in Figure 3. The red line and blue line represent the in-cylinder pressure of different IVCs. The red line indicates that the intake valve closes before 540 CA, while the blue line demonstrates that the intake valve closes at about 540 CA. The advantage is that fewer pumping losses can be achieved if IVC closes to 540 CA. However, the fresh air trapped in the inactive cycle is exhausted into the exhaust pipe because of the normal exhaust valve event, which would cause decreased efficiency of the three-way catalytic converter. For this situation, Jinxing Zhao et al. [5] proposed a novel strategy by connecting a branch pipe to the exhaust split pipe of inactive cylinders so as to guide the fresh air to flow from the inactive cylinders into the downstream of the catalyst convertor, which is suitable for the fixed CDA operation. However, this strategy is not applicable to the VCD operation, because all cylinders switch between deactivation and reactivation continuously.

For the valve strategy of low-pressure charge, the intake valves are deactivated during the inactive cycle, as shown in Figure 4. Only the residual exhaust gas is trapped in the cylinder. The trapped residual exhaust gas expands to a lower pressure when the piston moves towards the bottom dead center (BDC), which may result in an undesired entry of lubricant into the combustion chamber of the inactive cycle. Moreover, when the exhaust valve opens normally in the exhaust stroke of the inactive cycle, the exhaust gases of the exhaust manifold would flow back to the inactive cylinder due to the
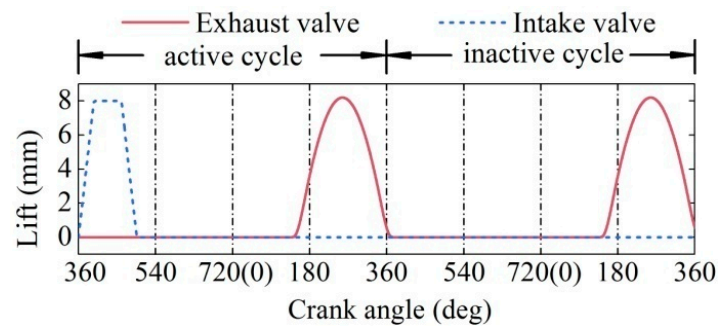
lower in-cylinder pressure, making the in-cylinder pressure rise to atmospheric pressure immediately, as shown in Figure 5, and thus resulting in more pumping losses during the inactive cycle.
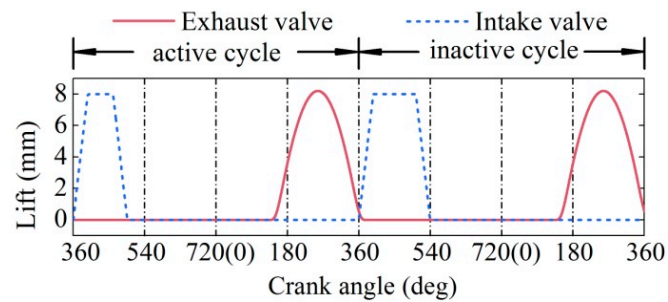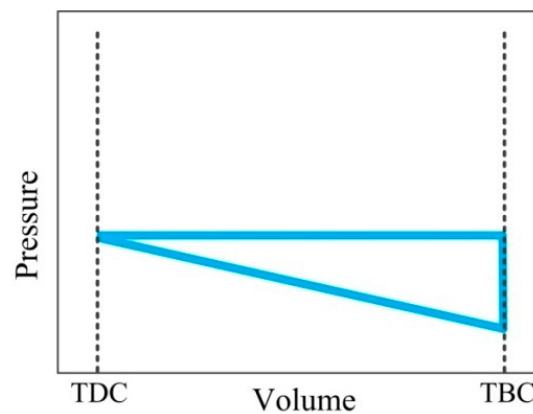
Figure 2. The schematic of the valve strategy based on fresh air trapping.

**Figure 3.** The schematic of in-cylinder pressure during the inactive cycle.

Figure 4. The schematic of the valve strategy based on low-pressure charge.

Figure 5. The schematic of in-cylinder pressure during the inactive cycle.

The valve strategy of fresh air trapping involves fewer pumping losses, but may cause high exhaust oxygen because the exhaust valve opens normally in the exhaust stroke of the inactive cycle. If the fresh air is replaced with exhaust gas, high exhaust oxygen would be avoided and less pumping losses can be achieved. Meanwhile, the shortcomings of the low-pressure charge can also be overcome. The valve strategy of exhaust gas trapping is proposed based on EMIV, as shown in Figure 6. The intake valve opens from the exhaust stroke of the last active cycle to the intake stroke of the inactive cycle. Therefore, a part of the exhaust gas is first pressed into the intake manifold, and then sucked into the cylinder, mixing with a small amount of fresh air. At the end of the inactive cycle, the trapped gas is discharged into the exhaust pipe. In this process, the key is to reduce the amount of oxygen sucked into the inactive cycle. In the paper, the mass fraction of oxygen in the exhaust pipe is recommended to be less than 1% in order to avoid the reduction in efficiency of the three-way catalytic converter. In addition, for the gas trapped in the inactive cycle, the in-cylinder pressure should be guaranteed to be greater than the minimum in-cylinder pressure limit, which is set at 0.02 MPa, according to Gottschalk's investigation [19].
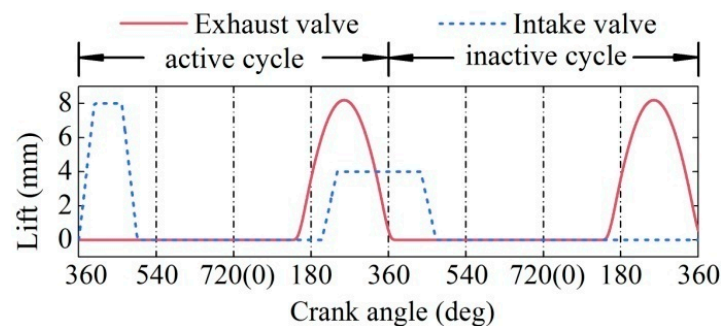
Figure 6. The schematic of the valve strategy based on exhaust gas trapping.

The VCD valve strategy based on EMIV allows each cylinder to switch between deactivation and reactivation with the firing density varying from 50 to 100% continuously, which is different from the fixed CDA mode when the inactive cylinders always never work. For the proposed valve strategy, the exhaust gas is directly discharged from the cylinder into the intake runner, and then sucked into the cylinder together with the fresh air during the inactive cycle. During this process, the VCD performances are affected by the IVO and IVC. For example, if the intake valve closes early, less trapped gas of the inactive cycle may lead to lower in-cylinder pressure and oil suction. Meanwhile, more exhaust gases are left in the intake manifold, which results in insufficient fresh air in the next active cycle. In the paper, energy loss in the transition period, the mass fraction of oxygen in the exhaust pipe, the minimum in-cylinder pressure of the active cycle, and the exhaust gas recirculation (EGR) rate of the active cycle have been analyzed at the level of the engine cycle with different intake valve opening timings and closing timings. The goal is to obtain the optimal IVO and IVC with the minimal energy losses on the premise of avoiding oil suction and high exhaust oxygen.

3. Model Details

3.1. 1D Model Validation

The study of the VCD is based on a four-cylinder gasoline engine of a SAIC Motor with a double variable valve train (DVVT), and the main parameters of the prototype engine are listed in Table 1.

The 1D prototype engine model is constructed and calibrated using experimental data in GT-Power. In the simulation model, the WoschniGT model is adopted to simulate the heat transfer processes, and the formula is shown as below:

$$h_c = 3.26B^{-0.2}p^{0.8}T^{-0.55}w^{0.8} \tag{1}$$

where h_c is the heat transfer coefficient, B is the bore of cylinder, p is the instantaneous cylinder pressure, T is the mean cylinder gas temperature, and w is the average cylinder gas velocity. The engine friction is calculated using the Chen-Flynn engine friction model, as shown in Equation (2).

$$FMEP = FMEP_{Const} + AP_{Cyl.max} + Bc_{p.m} + Cc^2_{p.m} \tag{2}$$

where $FMEP_{Const}$ is the constant part of FMEP, A is the peak cylinder pressure factor, B is the mean piston speed factor, C is the mean piston speed squared factor, $P_{Cyl.max}$ is the maximum cylinder pressure, and $c_{p.m}$ is the mean piston speed. The accuracy of the model under full load condition is validated through the experiments of the prototype engine, as shown in Figure 7. Data analyses demonstrate that the prediction error of the model is less than 5% under full load condition. In a GT-Power environment, heat transfer losses and friction losses are calculated based on every cylinder pressure. The heat transfer losses and friction losses are the sum of each cylinder's contributions. For the VCD operation, heat transfer losses and friction losses are reduced compared to normal engine operation due to the lower pressure of some inactive cylinders. Therefore, the WoschniGT model and the Chen-Flynn friction model are feasible for the VCD engine model.

Table 1. Engine specifications.

|	
Engine type	L4
Displacement	1.8 L
Valve train	DVVT
Number of valves	4 per cylinder
Stroke/Bore	89.3 mm/80 mm
Connecting rod length	133.1 mm
Compression ratio	10.5
Rated power	95.7 kW @ 6000 r/min
Rated torque	171.3 N·m @ 4500 r/min
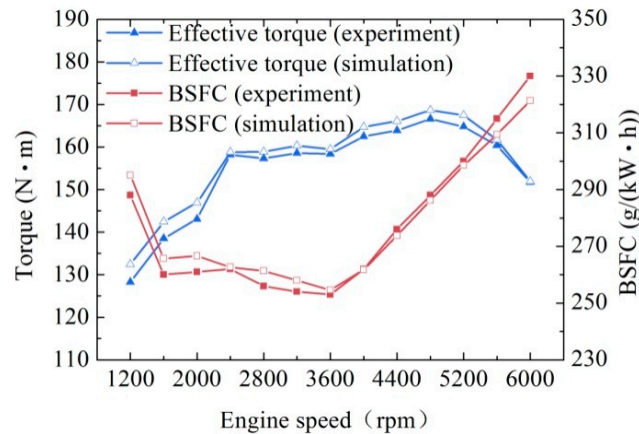
Figure 7. Comparisons of simulations and experiments under full load condition.

In this study, VCD is mainly discussed at 1200 rpm and 1600 rpm, and the comparisons of the BMEP and the brake specific fuel consumption (BSFC) between the simulation results and the experiment results are presented in Figure 8. The errors of BMEP and BSFC are also less than 5%. Therefore, the target engine model can be established based on the simulated prototype engine with high accuracy in the prediction of engine performances. In order to analyze VCD performances with the EMIV, the 1D model with the EMIV is established in GT-Power by replacing the valve train of prototype engine model with the template ValveSolSignalConn controlled via a logic signal (0 or 1), as shown in Figure 9. The valve will start opening or closing when the control signal switches between 0 and 1, which provides a method to simulate VCD performances with the EMIV.
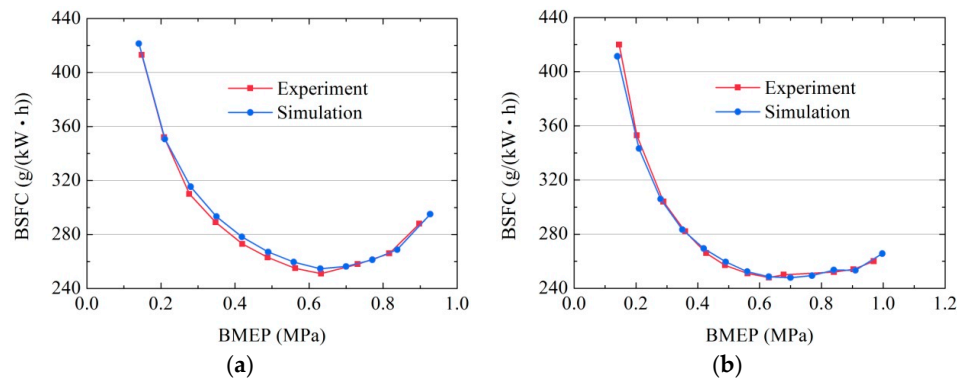
Figure 8. Comparisons of simulation results and experimental results at 1200 rpm and 1600 rpm: (**a**) 1200 rpm; (**b**) 1600 rpm.
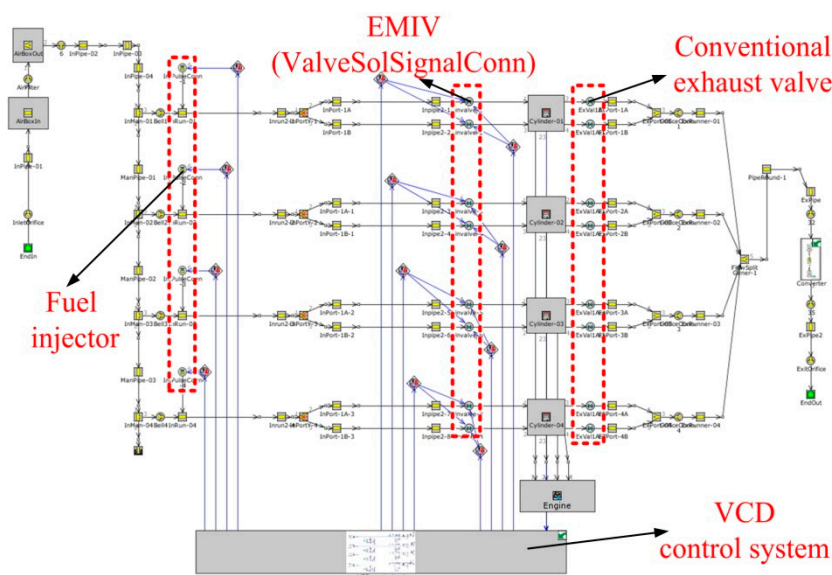
Figure 9. 1D model with EMIV.

3.2. VCD Model Validation Using 3D Code

Although the proposed valve strategy with exhaust gas trapped can achieve VCD operation, high exhaust oxygen is likely to occur if the intake valves close late. In order to accurately analyze the distribution of exhaust gas and fresh air in the intake manifold when the intake valves open at exhaust stroke, the discretization length of pipes in the 1D model of the VCD based on the EMIV is tuned using the simulation results of the 3D calculations.

Discretization refers to splitting large parts into smaller sections to improve the accuracy of the model in GT-Power. For engine cycle simulation, a discretization length of approximately 0.4 times the cylinder bore diameter is recommended for the intake system and 0.55 times the bore is recommended for the exhaust system. For the VCD operation with the proposed valve strategy, the exhaust gas pushed into the intake manifold would be mixed with fresh air, and the mixed gas is not homogeneous. However, larger discretization lengths of the 1D model will normally result in great errors. Therefore, the 3D code is used to calibrate the discretization lengths of the 1D model. The 3D model coupled with the 1D engine model is used to analyze the mixing process of the exhaust gas and fresh air. In order to reduce the co-simulation computational cost, only the intake manifold of one cylinder is adopted in the co-simulation in FLUENT, and the corresponding 1D-3D co-simulation model is shown in Figure 10. In the co-simulation model, 1D data from GT-Power are used for the boundary conditions of the 3D model, and the results of FLUENT are also received by GT-Power.
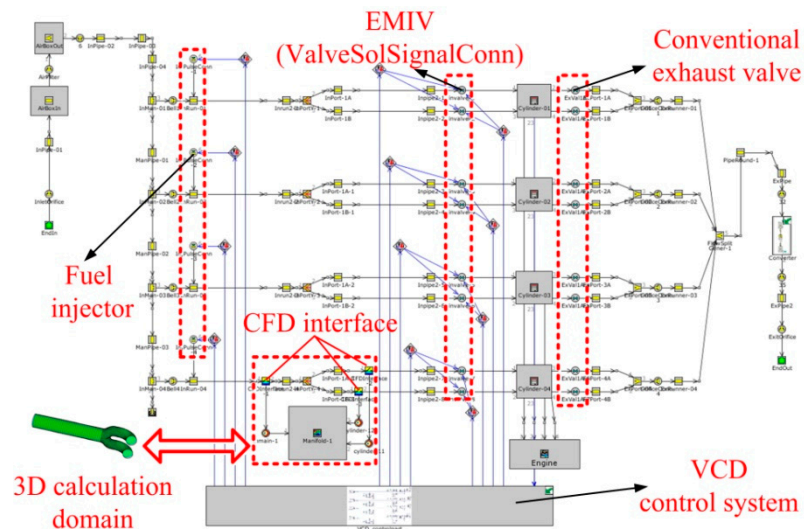
Figure 10. 1D-3D co-simulation model.

3.2.1. Results of 3D Code

The active cycles preferentially work in high efficiency area in order to improve fuel economy. So the 0.71 MPa of gross indicated mean effective pressure (IMEP360) with minimum indicated specific fuel consumption (ISFC) at 1200 rpm for prototype engine, as shown in Figure 8, is chosen for active cycle to compare the mass fraction of carbon dioxide between 3D model and 1D model. Figure 11 shows the mass fraction of carbon dioxide and oxygen of 3D calculated results when the intake valve opens at 180 CA and closes at 415 CA. To a certain extent, the mass fraction of carbon dioxide and oxygen represent the distribution of exhaust gas and fresh air, respectively. It can be observed that the exhaust gas is continuously pressed into the intake manifold while the fresh air flows back gradually from 180 CA to 360 CA (TDC). After 360 CA, the exhaust gas is sucked into the inactive cylinder until intake valves close at 415 CA. Since then the distribution of exhaust gas and fresh air changes slowly. As we can see, there is an obvious transition layer between the exhaust gas and the fresh air in the gas mixing process. So most of the gas sucked into the inactive cylinder would be exhaust gas by reasonably controlling the IVC, which avoids high exhaust oxygen and low efficiency of the three-way catalytic converter.
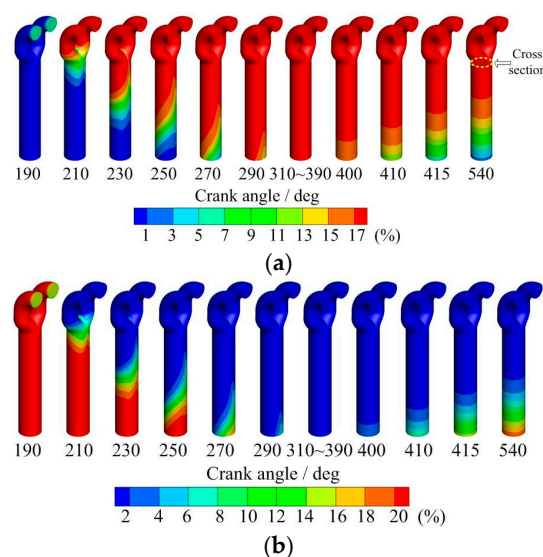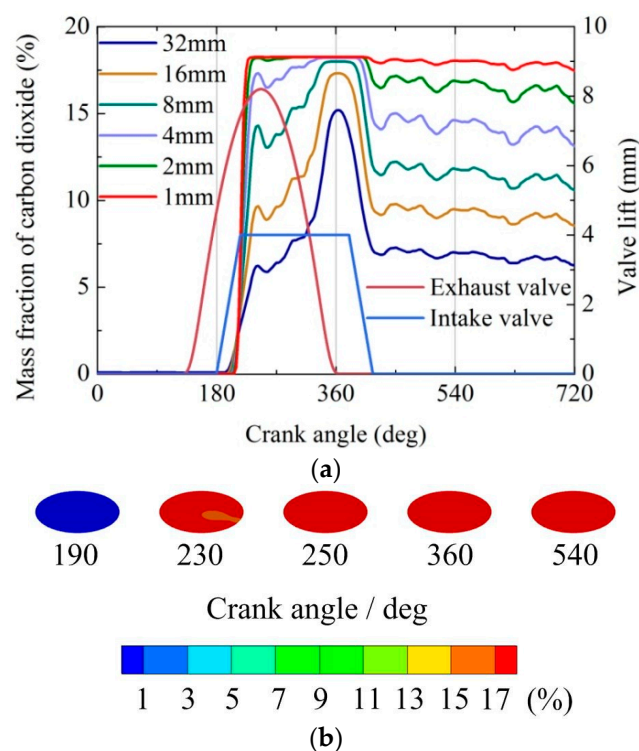

Figure 11. Mass fraction of carbon dioxide and oxygen in 3D simulation: (**a**) Mass fraction of carbon dioxide; (**b**) Mass fraction of oxygen.

3.2.2. Results of 1D Model

In the 1D model, the mass fractions of carbon dioxide of the 1D model with different discretization lengths on the giving cross-section shown in Figure 11a are presented in Figure 12a. A discretization length of 32 mm (0.4 * Bore) is the recommended value for the intake system. However, the mass fraction of carbon dioxide with 32 mm is different from the result of the co-simulation model. For example, the mass fraction of the 1D model at 270 CA is about 6.4%. Correspondingly, the value of the co-simulation model is about 17.7%. The main reason for the large difference is that the discretization length of 32 mm causes the mixed gas homogeneous in a discretized sub-volume with the length of 32 mm. For the 1D model, as the discretization length decreases to 1 mm, the mass fraction of carbon dioxide reaches the maximum value of 18.3% at 230 CA, and keeps this value until the intake valves close at 415 CA. During 415–540 CA, the mass fractions of carbon dioxide change slowly due to the free diffusion of molecules.

Figure 12. Mass fractions of carbon dioxide: (**a**) 1D simulation; (**b**) 3D calculation.

For the 3D code, the mass fractions of carbon dioxide on the giving cross-section shown in Figure 11a at different crank angles are presented in Figure 12b. As we can see, the mass fraction of carbon dioxide on the cross-section is less than 1% at 190 CA, which means that the exhaust gas does not reach the cross-section at the early stage. As the exhaust gas is continuously discharged into the intake runner, the mass fraction of carbon dioxide on most of the cross-section is about 17.7% at 230 CA, which indicates that the exhaust gas arrives at the cross-section. During 230–360 CA, the exhaust gas is continuously discharged into the intake manifold, and the mass fraction of carbon dioxide on the cross-section is kept at 17.7%. Since the intake valve closes at 415 CA, the mass fraction of carbon dioxide changes slowly because some exhaust gas still remains on the cross-section.

The simulation results show that the mass fractions of carbon dioxide reach the maximum value at 230 CA for both the 1D model (discretization length of 1 mm) and the 3D code. The error of the maximum value is about 3%. After 230 CA, the mass fractions of carbon dioxide remain unchanged. In the whole process, the mass fraction changes with a discretization length of 1 mm are consistent

with the corresponding results of the 3D calculation. Finally, the discretization length in the 1D VCD model based on EMIV is tuned to 1 mm.

4. Results and Discussion

In this section, the studies of the VCD operation are based on the tuned 1D model above. The aim is to discuss the energy losses of the VCD operation, the minimum in-cylinder pressure of the inactive cycle, and the mass fraction of oxygen in the exhaust pipe to obtain the optimal IVO and IVC of the proposed valve strategy. The IMEP360 values of 0.71 MPa and 0.78 MPa with a corresponding minimum ISFC of 1200 rpm and 1600 rpm for the prototype engine are selected, respectively, as the operation points for the active cycle.

4.1. Energy Losses during the Transition Process

When the engine operates under VCD condition, each cylinder switches between the active cycle and the inactive cycle frequently. Energy losses during the deactivation and reactivation of the cylinders have a significant impact on the brake thermal efficiency of the engine. Figure 13 shows an example of the pressure-volume (PV) during one inactive cycle and one active cycle when the intake valves open at 180 CA and close at 420 CA. During the transition from the active cycle to the inactive cycle, energy losses are mainly consumed in two periods including gas exchange from exhaust stroke of the active cycle to intake stroke of the inactive cycle (Period I) and the two-stroke compression and expansion process of the inactive cycle (Period II). In the paper, the energy losses during the transition process are analyzed under the VCD operation of one active cycle followed by one inactive cycle (50% firing density).
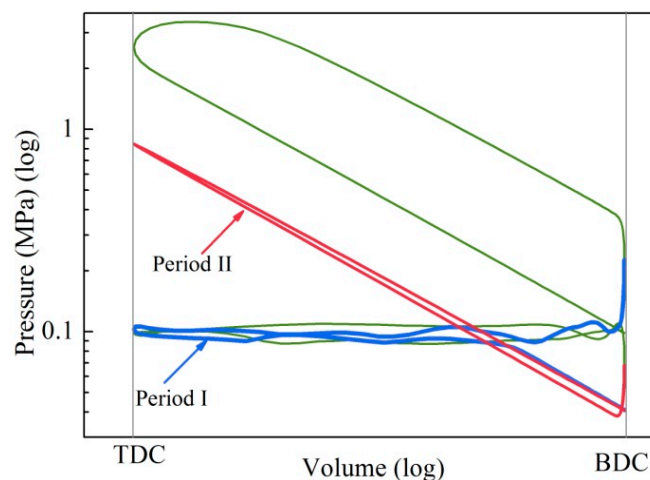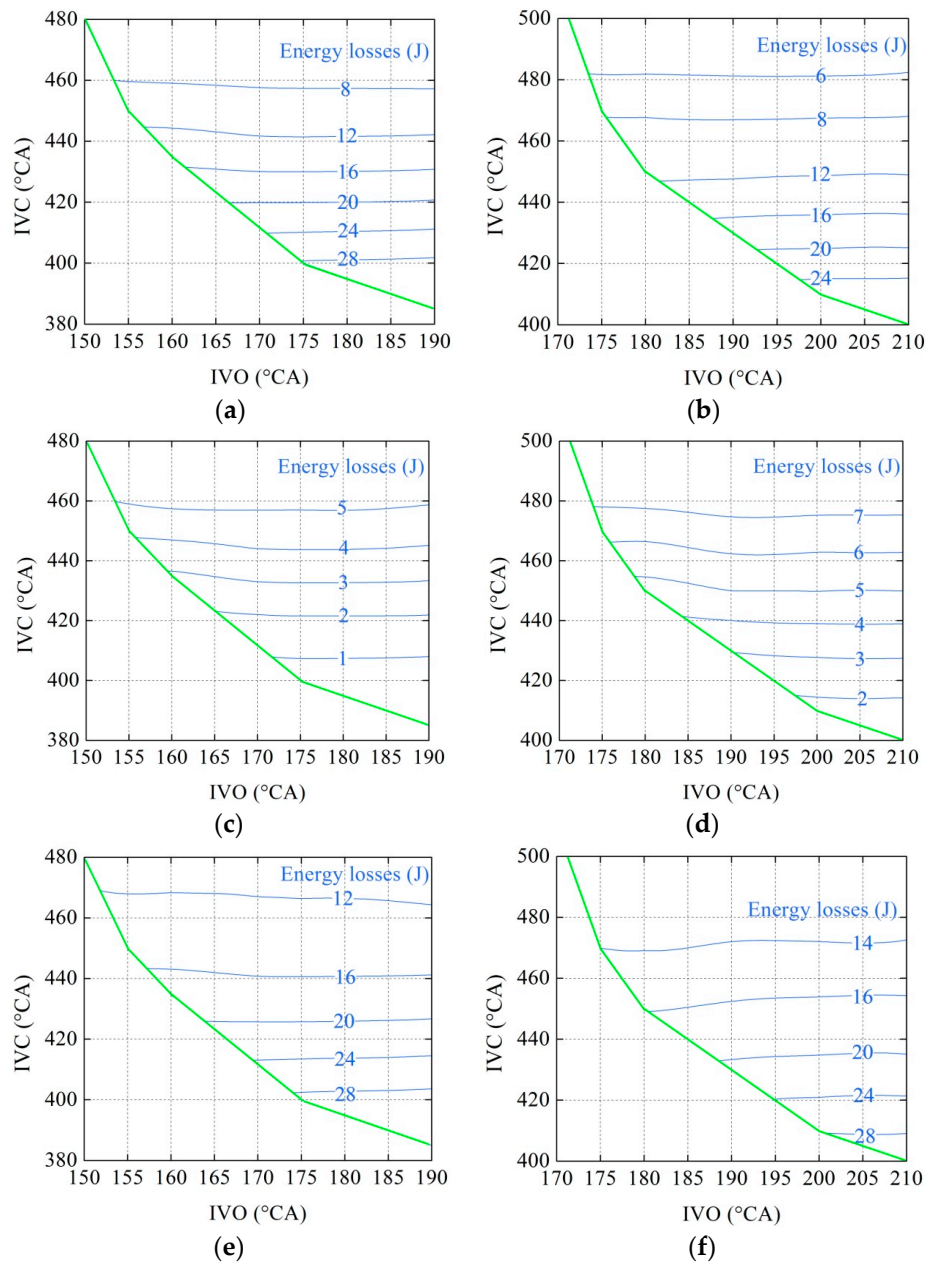

Figure 13. The in-cylinder pressure of one inactive cycle and one active cycle.

Figure 14 shows the energy losses of Period I and Period II with a different IVO and IVC. In the area below the green line, the large amount of exhaust gas remaining in the intake manifold leads to an insufficient fresh air charge of the active cycle, so there are no data in this area for Figure 14 and the following figures. This will be explained in Section 4.3.

The energy losses of Period I (see Figure 14a,b) decrease with the delay of the IVC, because delaying the IVC causes a decrease in in-cylinder pressure later and the area of the pressure curve in Period I is reduced. In Period II, the cylinder goes through the compression stroke and expansion stroke. The pressure during the expansion stroke is less than that during the compression stroke due to heat transfer. The energy losses of Period II increase with the delay of IVC (see Figure 14c,d). This is due to the fact that the delaying IVC leads to more high temperature exhaust gas being sucked into the inactive cylinder, resulting in more heat transfer losses. Figure 14e,f show the total energy losses of Period I and Period II. It can be seen that delaying IVC is conductive to reducing

the total energy losses. Therefore, the intake valves should close later for the VCD operation from the perspective of energy losses.

Figure 14. The energy losses of two periods: (**a**) Period I at 1200 rpm; (**b**) Period I at 1600 rpm; (**c**) Period II at 1200 rpm; (**d**) Period II at 1600 rpm; (**e**) Total energy losses at 1200 rpm; (**f**) Total energy losses at 1600 rpm.

*4.2. Minimum In-Cylinder Pressure of the Inactive Cycle*

The lower in-cylinder pressure may result in an undesired entry of lubricant into the combustion chamber during the inactive cycle. For the proposed valve strategy, the minimum in-cylinder pressure of the inactive cycle at a different IVO and IVC is shown in Figure 15. The minimum in-cylinder pressure is proportional to the mass of the exhaust gas trapped in the inactive cycle, so the minimum in-cylinder pressure increases gradually with the delay of the IVC. In order to avoid oil suction, the intake valves need to close later than 417 CA and 423 CA, respectively, for 1200 rpm and 1600 rpm, in order to ensure that the minimum pressure is greater than 0.02 MPa.
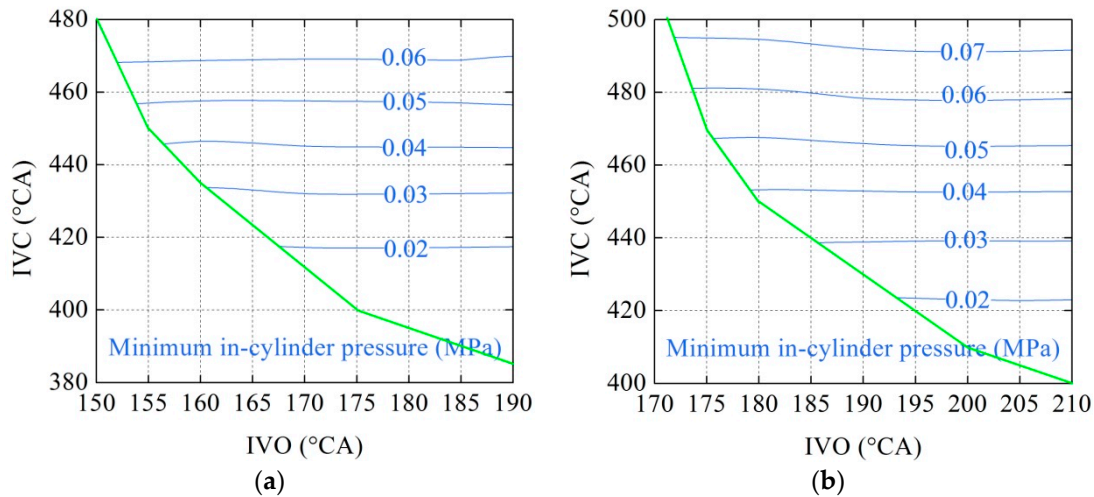
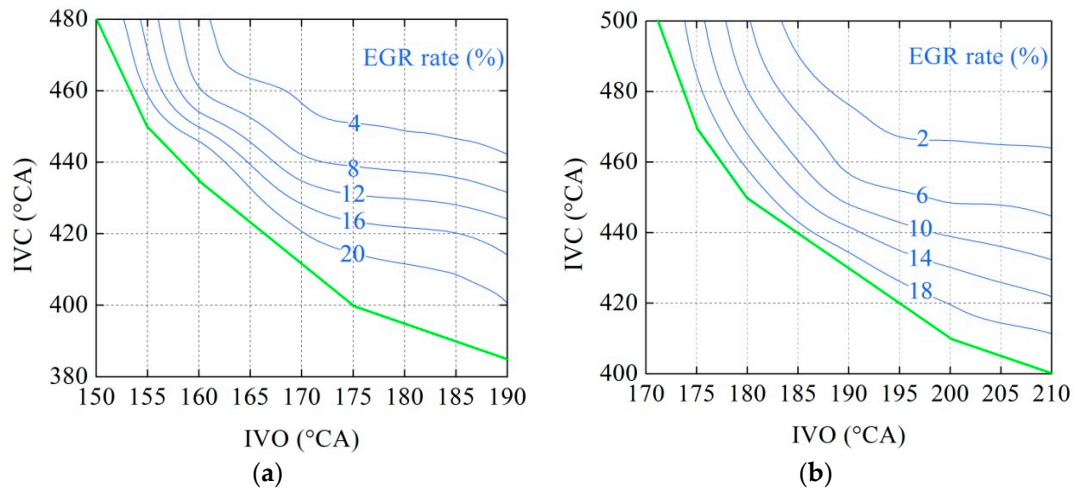**Figure 15.** The minimum in-cylinder pressure of the inactive cycle: (**a**) 1200 rpm; (**b**) 1600 rpm.

4.3. Mass Fraction of Oxygen in Exhaust Gas

Figure 16 shows the mass fraction of oxygen in the upstream of the catalyst convertor with a different IVO and IVC. It can be seen that delaying the IVC leads to an increase in the mass fraction of oxygen at the same IVO, which is due to more fresh air in combination with exhaust gas being sucked into the cylinder. Moreover, the mass fraction of oxygen decreases gradually as the firing density increases with the same IVO and IVC because the oxygen in the exhaust manifold is mainly from the inactive cycle. In Section 4.1, it is concluded that delaying the IVC is beneficial to the reduction of the total energy losses during the transition. Therefore, the IVC can be properly delayed to reduce energy losses as the firing density increases.
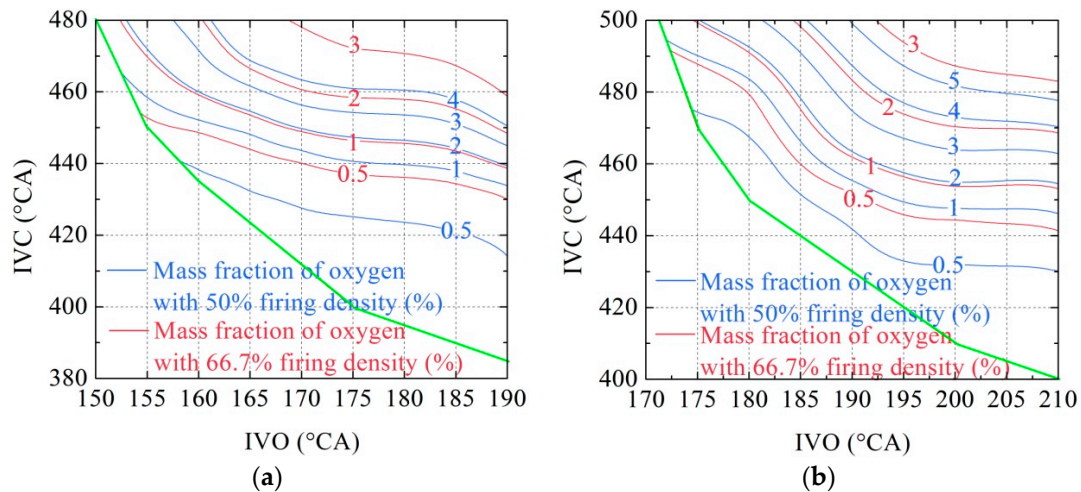
Figure 16. Mass fraction of oxygen in the upstream of catalyst convertor: (**a**) 1200 rpm; (**b**) 1600 rpm.

Figure 17 shows the EGR rate of the active cycle under VCD operations. It can be seen that the EGR rate increases with the advance of the IVO and IVC because more and more exhaust gas would remain in the intake manifold with the advance of the IVO and IVC. In the area below the green line, the large amount of exhaust gas that remained in the intake manifold during the inactive cycle leads to a high EGR rate and an insufficient fresh air charge in the active cycle, which is the reason why there are no data below the green line of the related figures in the full paper. Moreover, the change trends of the EGR rate are opposite to the mass fraction of oxygen. The high EGR rate means that more exhaust gas remains in the intake manifold and less fresh air is sucked into the inactive cycle, which results in a decrease in the mass fraction of oxygen, and vice versa.

Figure 17. The EGR rate of the active cycle: (**a**) 1200 rpm; (**b**) 1600 rpm.

4.4. Area of Optimal IVO and IVC

The energy losses during transition, the minimum in-cylinder pressure of the inactive cylinder, and the mass fraction of oxygen in the exhaust gas have been discussed above. Figure 18 shows the line of in-cylinder pressure (0.02 MPa) of the inactive cylinder and the line of mass fraction of oxygen (1%). On the premise of guaranteeing the mass fraction of oxygen under 1% and keeping the minimum in-cylinder pressure of the inactive cylinder above 0.02 MPa, the optimal areas for IVO and IVC can be determined by the variation features of energy losses during the transition process. Therefore, A1 and A2 are confirmed as the optimal area under the firing densities of 50% and 66.7%, respectively. As we can see, the energy losses in the optimal area decrease with the increase in firing density.
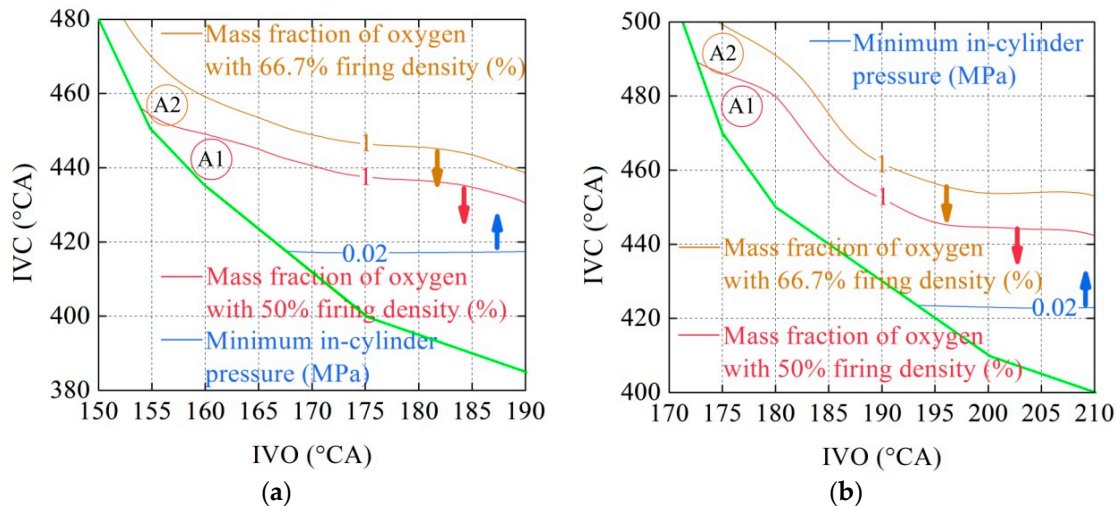

Figure 18. The optimal area of VCD operations: (**a**) 1200 rpm; (**b**) 1600 rpm.

4.5. Results at Higher Engine Speeds

Cylinder deactivation is mainly used to improve the fuel economy for low load conditions of low and middle engine speeds. The above discussions are focused on low engine speed. In order to verify the consistency of results at different engine speeds, the results at higher engine speeds (2400 rpm and 3200 rpm) are shown in Figure 19. The IMEP360 values of 0.88 MPa and 0.98 MPa are selected, respectively, as the operation points of the active cycle for 2400 rpm and 3200 rpm.
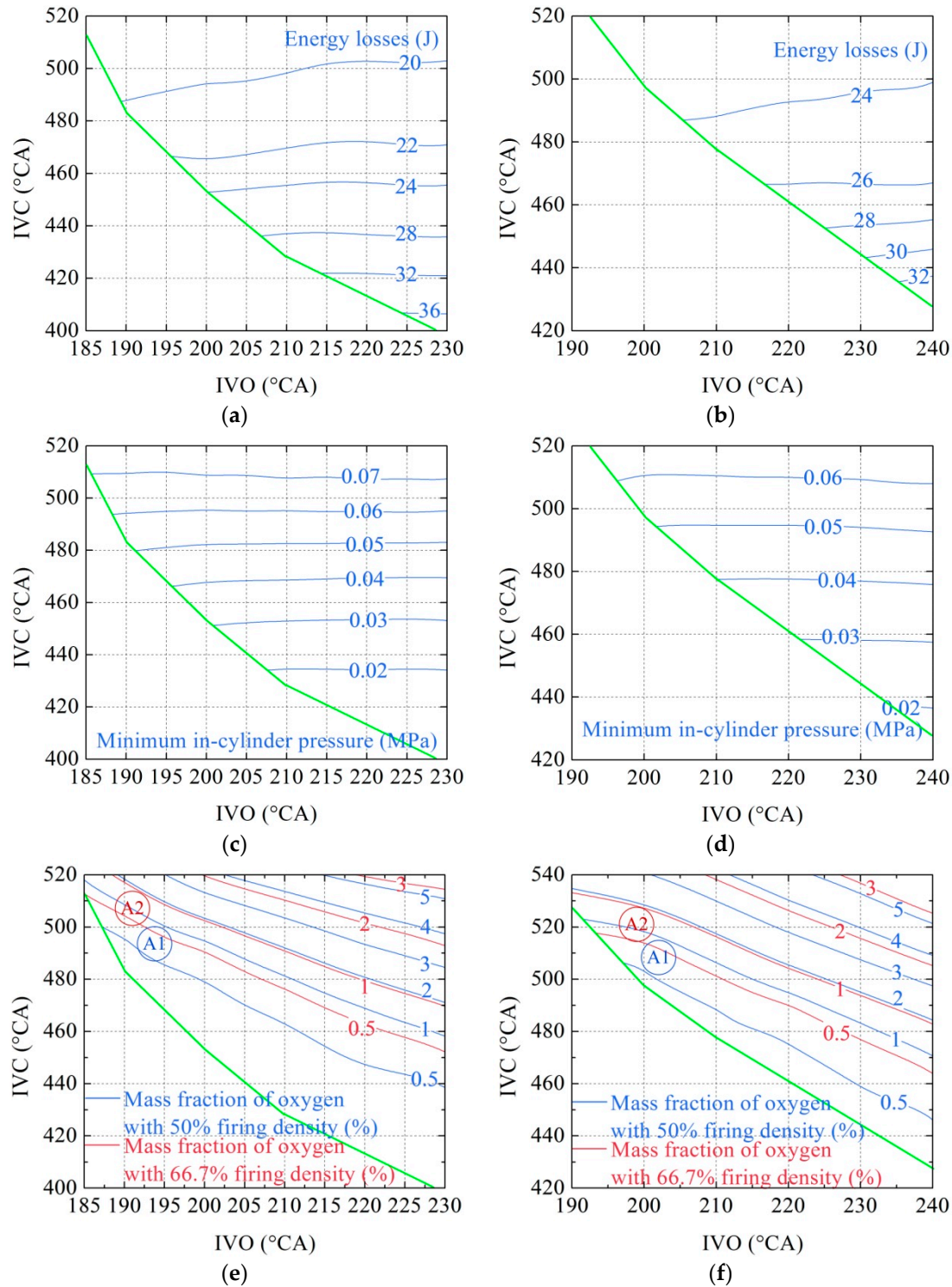
Figure 19. The results of 2400 rpm and 3200 rpm with the proposed VCD valve strategy: (**a**) Total energy losses at 2400 rpm; (**b**) Total energy losses at 3200 rpm; (**c**) The minimum in-cylinder pressure of the inactive cycle at 2400 rpm; (**d**) The minimum in-cylinder pressure of the inactive cycle at 3200 rpm; (**e**) Mass fraction of oxygen at 2400 rpm; (**f**) Mass fraction of oxygen at 3600 rpm.

As we can see, delaying the IVC is beneficial for reducing the total energy losses during the transition process and increasing the minimum in-cylinder pressure of the inactive cycle. For the mass fraction of oxygen, it also increases with the delay of IVC when the IVO is same. In addition, the mass fraction of oxygen decreases gradually as the firing density increases with the same IVO and IVC.

Under the same restrictions where the mass fraction of oxygen is under 1% and the minimum in-cylinder pressure of the inactive cylinder is above 0.02 MPa, the optimal areas (A1 and A2) for IVO and IVC are achieved, as shown in Figure 19e,f. Finally, we can see that the results at higher engine speeds are consistent with those at lower speeds.

4.6. Fuel Economy Benefits

Under low load condition, the PMEP is large for throttled engines due to lower intake pressure. Based on theEMIV, the EIVC strategy is adopted to control the amount of gas charge. Due to unthrottling, the PMEP is significantly reduced under low and medium load operations, as shown in Figure 20. When the engine works in VCD operations with the EIVC strategy, the PMEP of the firing cycle would be reduced further.
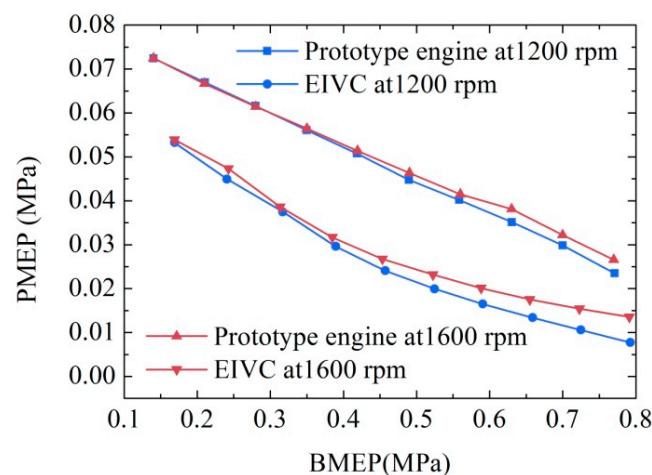

Figure 20. The PMEP of the prototype engine and the EIVC strategy.

Through the above analysis, the optimal area of the IVO and IVC can be obtained as the engine works under VCD operations. Figure 21 shows the PMEPs of the prototype engine, the EIVC strategy and VCD with EIVC in the same operating conditions. Due to the higher IMEP of the firing cycle, the PMEP of the VCD with EIVC is further reduced when compared to the EIVC strategy. However, the inactive cycle under VCD operation would consume energy, which reduces the improvement of fuel economy achieved by the VCD. Through the optimization of the IVO and IVC, the minimum total energy losses of the inactive cylinder during the transition process have been obtained.
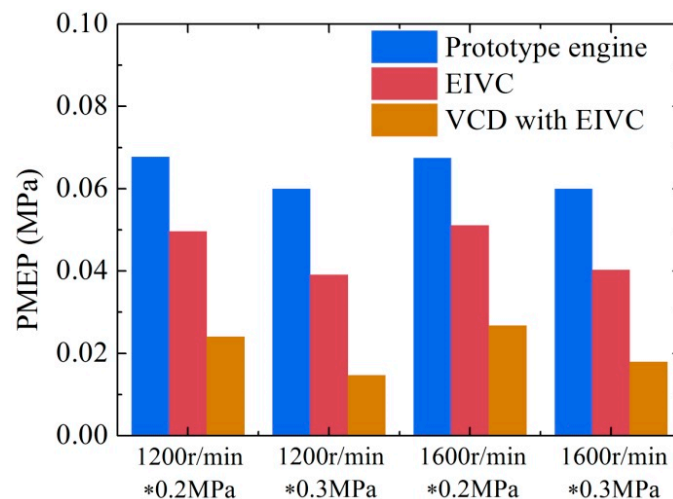

Figure 21. The PMEPs of the prototype engine, EIVC strategy and VCD with EIVC.

Finally, the fuel economy achieved by the VCD operations based on the EMIV with the EIVC strategy is illustrated in Figure 22. When the BMEP is lower than 0.3 MPa, the fuel economy achieved by the VCD strategy is better than that achieved by the EIVC strategy. At 1200 and 1600 rpm, the VCD strategy provides a 12.5–16.6% and 9.7–14.6% reduction in BSFC, respectively, compared with the prototype engine when the BMEP ranges from 0.3 MPa to 0.2 MPa.
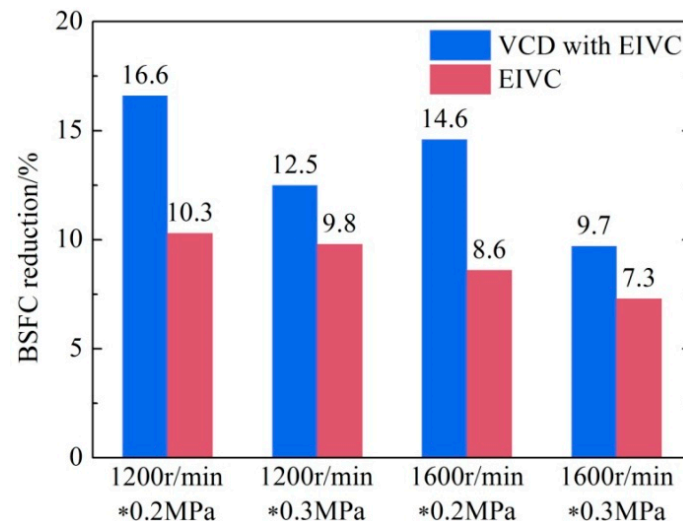

Figure 22. Benefits to fuel economy achieved by VCD operations.

5. Conclusions

In this paper, a new valve strategy with EMIV is proposed to realize VCD operation without any modification to the exhaust valves. The VCD model, which is established in GT-Power and tuned using the 3D code, is used to analyze the effects of the valve strategy on energy losses, in-cylinder pressure, and the mass fraction of oxygen in exhaust gas. The main conclusions are summarized below.

(1) When the exhaust gas is pressed into the intake manifold, there is a significant boundary layer between the exhaust gas and the fresh air. Through a reasonable control of the IVO and IVC, most of the gas sucked into the inactive cycle is the exhaust gas, which avoids not only high exhaust oxygen but also oil suction.

(2) Advancing the IVO and delaying the IVC helps to reduce the total energy losses and increase the minimum in-cylinder pressure of the inactive cycle, so as to avoid the risk of oil suction.

(3) On the premise of avoiding high exhaust oxygen and oil suction, the optimal areas for IVO and IVC can be determined by the variation features of energy losses during the transition process. The energy losses in the optimal area decrease with the increase in firing density.

(4) Under low load conditions, the fuel economy achieved by VCD is better than that of the EIVC strategy. At 1200 and 1600 rpm, fuel economy is improved 12.5–16.6% and 9.7–14.6%, respectively, compared to the prototype engine when the BMEP ranges from 0.3 MPa to 0.2 MPa.

References

1. Wilcutts, M.; Switkes, J.; Shost, M.; Tripathi, A. Design and benefits of dynamic skip fire strategies for cylinder deactivated engines. *SAE Int. J. Engines* **2013**, *6*, 278–288. [CrossRef]

2. Abas, M.; Martinez-Botas, R. Engine Operational Benefits with Cylinder Deactivation in Malaysian Urban Driving Conditions. In Proceedings of the SAE 2015 World Congress, Detroit, MI, USA, 21–23 April 2015.

3. Leone, T.G.; Pozar, M. Fuel economy benefit of cylinder deactivation—Sensitivity to vehicle application and operating constraints. *SAE Tech. Pap.* **2001**. [CrossRef]

4. Stabinsky, M.; Albertson, W.; Tuttle, J.; Kehr, D.; Westbrook, J.; Karbstein, H.; Kuhl, M. Active fuel management™ technology: Hardware development on a 2007 GM 3.9 L V-6 OHV SI engine. *SAE Tech. Pap.* **2007**. [CrossRef]

5. Zhao, J.; Xi, Q.; Wang, S.; Wang, S. Improving the partial-load fuel economy of 4-cylinder SI engines by combining variable valve timing and cylinder-deactivation through double intake manifolds. *Appl. Therm. Eng.* **2018**, *141*, 245–256. [CrossRef]

6. Millo, F.; Mirzaeian, M.; Luisi, S.; Doria, V.; Stroppiana, A. Engine displacement modularity for enhancing automotive si engines efficiency at part load. *Fuel* **2016**, *180*, 645–652. [CrossRef]

7. GreenCarCongress. Volkswagen to Implement Cylinder Deactivation in 4-Cylinder 1.4 TSI Engines in 2012. 2011. Available online: https://www.greencarcongress.com/2011/09/zas-20110902.html (accessed on 29 October 2018).

8. Fujiwara, M.; Kumagai, K.; Segawa, M.; Sato, R.; Tamura, Y. Development of a 6-cylinder gasoline engine with new variable cylinder management technology. *SAE Tech. Pap.* **2008**. [CrossRef]

9. Maehara, H.; Kitawaki, S.; Abe, T.; Saito, S.; Tsukui, T. Development of variable cylinder management system for large motorcycles-an effective way of reducing output change at switching of the number of working cylinders. *SAE Tech. Pap.* **2010**. [CrossRef]

10. Shiao, Y.J.; Dat, L.V. The Optimal Strategies for Improving Efficiency in Camless Engines. In Applied Mechanics and Materials. *Trans. Tech. Pub.* **2012**, *145*, 83–87. [CrossRef]

11. Li, T.; Gao, Y.; Wang, J.; Chen, Z. The Miller cycle effects on improvement of fuel economy in a highly boosted, high compression ratio, direct-injection gasoline engine: EIVC vs. LIVC. *Energy Convers. Manag.* **2014**, *79*, 59–65. [CrossRef]

12. Tomoda, T.; Ogawa, T.; Ohki, H.; Kogo, T.; Nakatani, K.; Hashimoto, E. Improvement of diesel engine performance by variable valve train system. *Int. J. Engine Res.* **2010**, *11*, 331–344. [CrossRef]

13. Millo, F.; Luisi, S.; Borean, F.; Stroppiana, A. Numerical and experimental investigation on combustion characteristics of a spark ignition engine with an early intake valve closing load control. *Fuel* **2014**, *121*, 298–310. [CrossRef]

14. Zhao, Y.; Zhou, B. Dynamic Cylinder Deactivation with Residual Heat Recovery. U.S. Patent Application No. 12/550,056, 3 April 2010.

15. Yüksek, L.; Özener, O.; Sandalcı, T. Cycle-skipping strategies for pumping loss reduction in spark ignition engines: An experimental approach. *Energy Convers. Manag.* **2012**, *64*, 320–327. [CrossRef]

16. Gosala, D.B.; Allen, C.M.; Shaver, G.M.; Farrell, L.; Koeberlein, E.; Franke, B.; Stretch, D.; McCarthy, J.J. Dynamic cylinder activation in diesel engines. *Int. J. Engine Res.* **2018**. [CrossRef]

17. Serrano, J.; Routledge, G.; Lo, N.; Shost, M.; Srinivasan, V.; Ghosh, B. Methods of evaluating and mitigating NVH when operating an engine in dynamic skip fire. *SAE Int. J. Engines* **2014**, *7*, 1489–1501. [CrossRef]

18. Liu, L.; Chang, S. Motion control of an electromagnetic valve actuator based on the inverse system method. *Proc. Inst. Mech. Eng. Part D J. Autom. Eng.* **2012**, *226*, 85–93. [CrossRef]

19. Gottschalk, W.; Fink, R.; Schultalbers, M. Investigations on Ventilation Strategies for SI Cylinder Deactivation Based on a Variable Valve Train. *SAE Tech. Pap.* **2016**. [CrossRef]